Climatic controls on individual ostracode stable isotopes in a desert lake: a modern baseline for Lake Turkana

Kaustubh Thirumalai[1], Andrew S Cohen[1], and Dustin Taylor[1]

[1]University of Arizona

December 7, 2022

Abstract

Stable carbon ($\delta^{13}C$) and oxygen ($\delta^{18}O$) isotope measurements in lacustrine ostracodes are widely used to infer past climatic conditions. Previous work has used individual ostracode valves to resolve seasonal and subdecadal climate signals, yet environmental controls on geochemical variability within co-occurring specimens from modern samples are poorly constrained. Here we focus on individual ostracode valves in modern-aged Lake Turkana sediments, an alkaline desert lake in tropical East Africa. We present individual ostracode valve analyses (IOVA) of $\delta^{13}C$ and $\delta^{18}O$ measurements (n = 329) of extant species Sclerocypris clavularis from 17 sites spanning the entire lake (n-avg ˜19 specimens per site). We demonstrate that the pooled statistics of individual valve measurements at each site overcome inter-specimen isotopic variance and are driven by hydrological variability in the lake. Mean IOVA-$\delta^{13}C$ and -$\delta^{18}O$ across the sites exhibit strong spatial trends with higher values at more southerly latitudes, modulated by distance from the inflow of the Omo River. Whereas the latitudinal $\delta^{13}C$ gradient reflects low riverine $\delta^{13}C$ and decreasing lacustrine productivity towards the southern part of the lake, the $\delta^{18}O$ gradient is controlled by evaporation superimposed on the waning influence of low-$\delta^{18}O$ Omo River waters, sourced from the Ethiopian highlands. We show that ostracode $\delta^{18}O$proximal to Omo River inflow is deposited under near-equilibrium conditions and that inter-specimen $\delta^{18}O$ variability across the basin is consistent with observed temperature and lake water $\delta^{18}O$ variability. IOVA can provide skillful constraints on high-frequency paleoenvironmental signals and, in Omo-Turkana sediments, yield quantitative insights into East African paleohydrology.

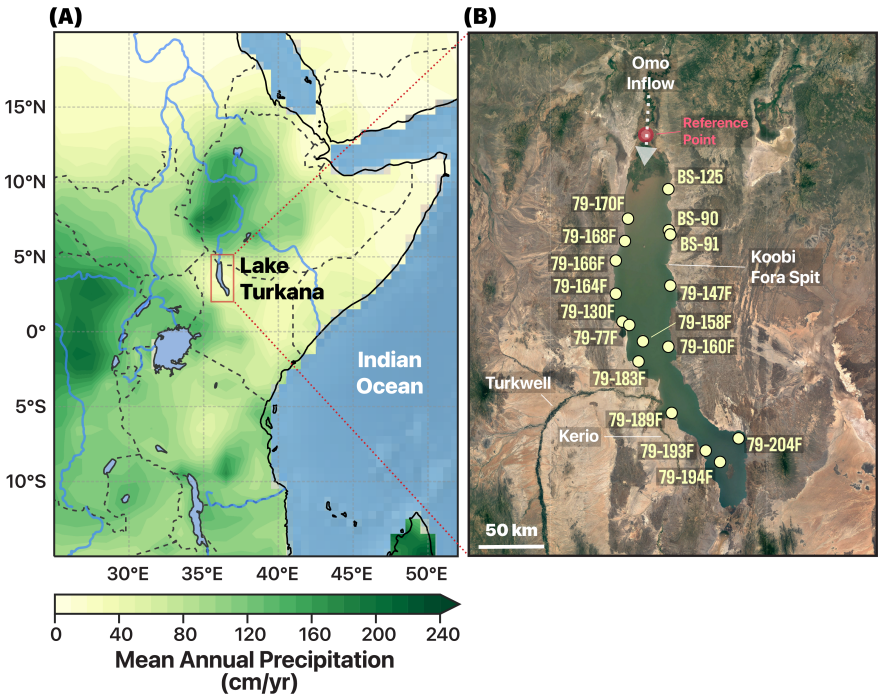

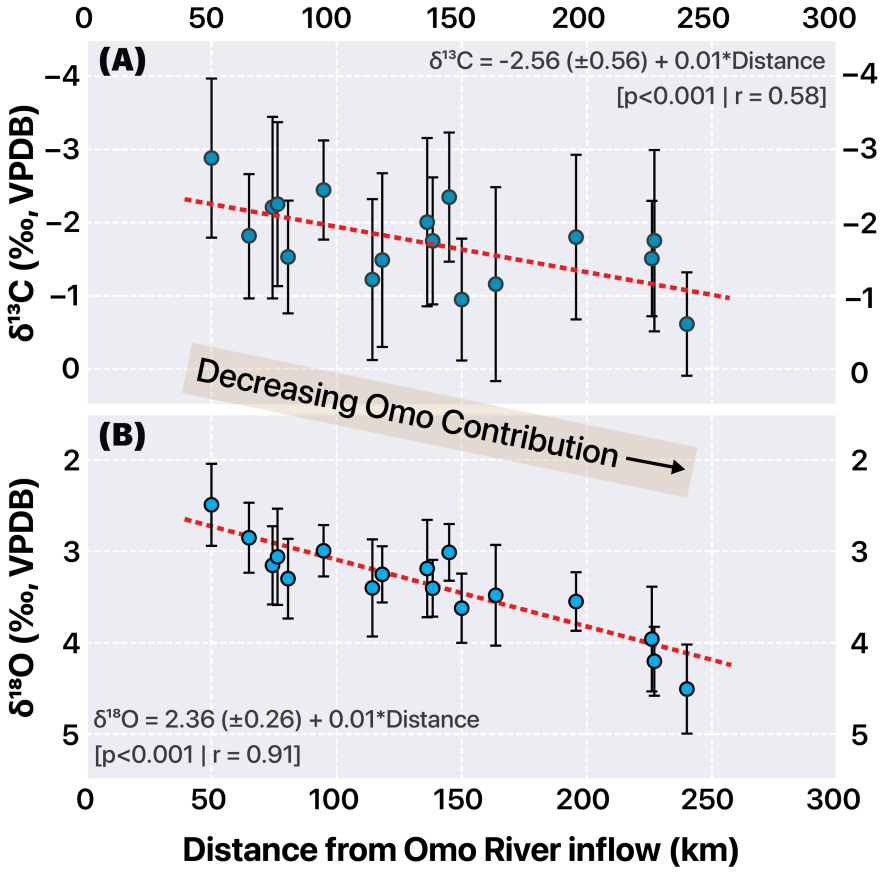

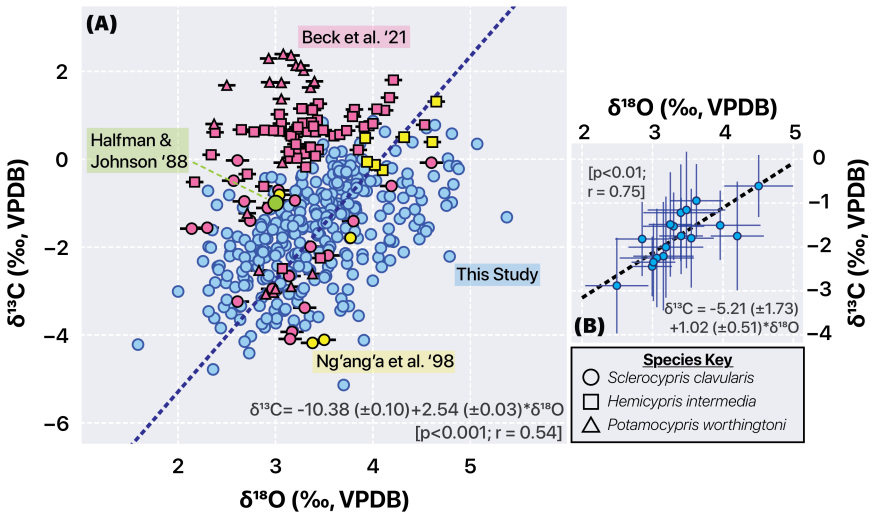

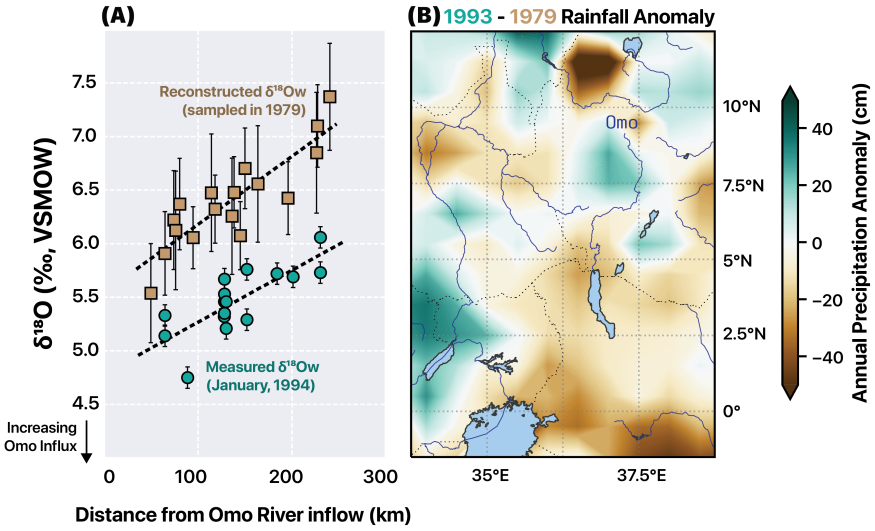

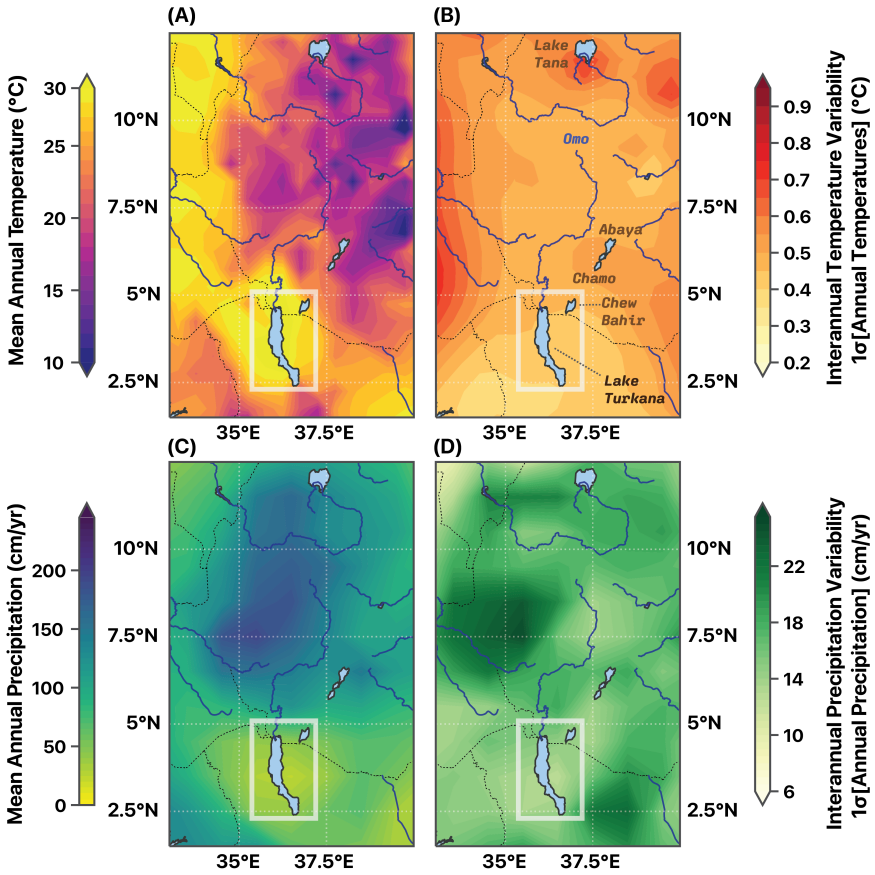

Climatic controls on individual ostracode stable isotopes in a desert lake: a modern baseline for Lake Turkana

K. Thirumalai[1], A. S. Cohen[1], D. Taylor[1]

[1] Department of Geosciences, University of Arizona, 1040 E. 4th Street Tucson, AZ 85721 United States of America

Corresponding author: Kaustubh Thirumalai (kaustubh@arizona.edu)

Key Points:

- We present a calibration of individual ostracode valve analyses (IOVA) of $\delta^{18}O$ and $\delta^{13}C$ of *S. clavularis* in modern Lake Turkana sediments.
- We find that Omo River inflow controls the pooled statistics of IOVA $\delta^{18}O$ and $\delta^{13}C$ across sites.
- $\delta^{18}O$ values of *S. clavularis* are consistent with effective calcite precipitation under near-equilibrium conditions.

Abstract

Stable carbon ($\delta^{13}C$) and oxygen ($\delta^{18}O$) isotope measurements in lacustrine ostracodes are widely used to infer past climatic and paleolimnological conditions. Previous work has used individual ostracode valves to resolve seasonal and subdecadal climate signals, yet environmental controls on geochemical variability within co-occurring specimens from modern samples are poorly constrained. Here we focus on individual ostracode valves in modern-aged Lake Turkana sediments, an alkaline desert lake in tropical East Africa. We present individual ostracode valve analyses (IOVA) of $\delta^{13}C$ and $\delta^{18}O$ measurements (n = 329) of extant species *Sclerocypris clavularis* from 17 sites spanning the entire lake (n_{avg} = ~19 specimens per site). We demonstrate that the pooled statistics of individual valve measurements at each site overcome inter-specimen isotopic variance and are driven by hydrological variability in the lake. Mean IOVA-$\delta^{13}C$ and -$\delta^{18}O$ across the sites exhibit strong spatial trends with higher values at more southerly latitudes, modulated by distance from the inflow of the Omo River. Whereas the latitudinal $\delta^{13}C$ gradient reflects low riverine $\delta^{13}C$ and decreasing lacustrine productivity towards the southern part of the lake, the $\delta^{18}O$ gradient is controlled by evaporation superimposed on the waning influence of low-$\delta^{18}O$ Omo River waters, sourced from the Ethiopian highlands. We show that ostracode $\delta^{18}O$ proximal to Omo River inflow is deposited under near-equilibrium conditions and that inter-specimen $\delta^{18}O$ variability across the basin is consistent with observed temperature and lake water $\delta^{18}O$ variability. IOVA can provide skillful constraints on high-frequency paleoenvironmental signals, and in Omo-Turkana sediments, yield quantitative insights into East African paleohydrology.

Plain Language Summary

Ostracodes are microscopic, aquatic crustaceans that deposit shells ('valves') made of calcium carbonate. Retrieved from sediment cores, these valves are widely used to estimate past water conditions using their shell chemistry. Here we focus on stable oxygen and carbon isotopes in numerous, individual valves in modern sediments taken from multiple sites across Lake Turkana, Kenya. This lake is located in a hot and arid region in equatorial East Africa. The major river that drains into Lake Turkana is the Omo River, which is sourced from rainfall in the Ethiopian Highlands. We find that ostracode stable isotopes are excellent recorders of lake hydrology in this basin and reveal a strong influence of the influx of Omo River waters. Analyzing several valves at each site helps overcome non-environmental controls on ostracode stable isotopes and allows for more accurate estimates of past water conditions. Our results provide a modern baseline of ostracode stable isotopes at Lake Turkana. We suggest that both the average of, and variations within individual-valve measurements of ostracode geochemistry can help characterize past hydrological variability and lake water conditions.

1. Introduction

The geochemistry of lacustrine ostracode shells has provided key insights into continental paleoclimatic fluctuations across the Phanerozoic eon. Stable carbon ($\delta^{13}C$) and oxygen ($\delta^{18}O$) analyses[†] of calcareous ostracode valves found in lake sediments have been used to reconstruct

[†] Stable isotopes in this work are reported using the standard δ notation: $\delta_x = \left(\frac{R_x}{R_{std}} - 1\right) \times 1000$, where *R* is the ratio of the abundance of the rare versus abundant isotope, *x* is the sample, and *std* is a reference standard. Here,

mean variations in past productivity, temperature, riverine inflow, and chemical composition of lake waters, as well as their links with regional hydroclimate change (Last et al., 1994; Palacios-Fest et al., 1994; Dixit et al., 2014; Pérez et al., 2013; Dettman et al., 1995; Dettman et al., 2005).

Conventionally, several ostracode valves from the same sedimentary interval are combined to generate a single measurement ("multi-specimen analysis"), whose value is thought to reflect the average ostracode isotopic composition across the timespan represented by that sample (Dixit et al., 2015; Escobar et al., 2010). However, it is well-known that ostracode calcification occurs rapidly, on the order of hours to days (Turpen & Angell, 1971; Chivas et al., 1986; Roca & Wansard, 1997) – timescales much smaller than the seasonal to centennial duration encompassed in a typical lacustrine time-averaged sample (Holmes, 2008). Multiple studies have investigated sample-size limitations associated with this approach, either through replicate multi-specimen analyses or via numerous measurements of individual ostracode valves ("individual ostracode valve analyses", abbreviated hereafter as IOVA) and have uncovered substantial geochemical variance amongst co-occurring specimens (Dixit et al., 2015; Palacios-Fest & Dettman, 2001; Holmes et al., 1995; Von Grafenstein et al., 1999; Schwalb et al., 2002; Heaton et al., 1995; Holmes, 2008). Citing both non-equilibrium effects as well as the short-lived duration of ostracode calcification relative to sample resolution, these findings called for the combination of large numbers of individual valves (n>15) in multi-specimen measurements to robustly reconstruct mean environmental conditions within a stratigraphic interval (Xia et al., 1997; Palacios-Fest & Dettman, 2001; Holmes, 2008; Escobar et al., 2010; Dixit et al., 2015).

On the other hand, few studies have taken advantage of the potential for rapidly deposited ostracode calcite to sample higher frequency subdecadal signals such as seasonality or interannual variability of lake temperature and hydrology. Notably, Dettman et al. (1995) measured individual-valve stable isotopes of various early- to mid-Holocene ostracode species in Lake Huron sediments to identify cold-season $\delta^{18}O$ extremes within sampled intervals. Escobar et al. (2010) applied individual ostracode-valve analyses of $\delta^{18}O$ (IOVA-$\delta^{18}O$) in *Cytheridella ilosvayi* specimens from lake sediments of the Yucatán Peninsula to constrain subdecadal hydrological variability across various late Holocene periods. More recently, Dixit et al. (2015) measured individual *Cyprideis torosa* valves in early Holocene intervals of paleolake Riwasa sediments in northern India and suggested that IOVA-$\delta^{18}O$ variance resulted from seasonal temperature and monsoon-driven hydroclimatic fluctuations. Collectively, these studies found intervals of large IOVA-$\delta^{18}O$ variance (interpreted to be environmentally mediated), ranging from ~5-15 ‰. Yet, to our knowledge, no study has conducted a systematic modern calibration between IOVA-$\delta^{18}O$ and observed lake conditions to investigate the fidelity of this approach in reconstructing high-frequency climate variability.

In this work, we report IOVA-$\delta^{18}O$ and -$\delta^{13}C$ in *Sclerocypris clavularis,* a relatively large, benthic ostracode that occurs commonly throughout Lake Turkana (Cohen, 1986). Our specimens from modern Lake Turkana sediments were collected from 17 different sites around the lake (Fig. 1B). Our main aims are to 1) characterize within-site isotopic variance across our individual measurements and compare pooled IOVA statistics across the basin, 2) investigate oxygen isotope equilibrium in ostracode calcite at Lake Turkana, 3) provide a modern stable isotope baseline at Lake Turkana as a benchmark for future studies utilizing IOVA, and 4)

values are reported in permil (‰) relative to the Vienna Pee Dee Belemnite (VPDB) reference for $\delta^{18}O$ and $\delta^{13}C$, whereas $\delta^{18}O$ of waters are reported relative to Vienna Standard Mean Oceanic Water (VSMOW).

explore the potential of this tool for inferring past hydrologic conditions within the lake and its watershed.

2. Climatic and Hydrological Setting

Lake Turkana, one of the great East African Rift Valley lakes, is a closed-basin system (*i.e.,* no direct outflow) situated in an arid region of equatorial eastern Africa. On average, the region receives less than ~25 cm of rainfall per year (Fig. 1). In contrast, the Ethiopian highlands located to the north, are much wetter, with upwards of 150 cm of average rainfall per year (Fig. 2C). Sourced in these highlands, the perennial Omo River comprises the major (>80-90 %) riverine inflow for Lake Turkana, with the Kerio and Turkwell rivers on the southern side being minor contributors (Avery & Tebbs, 2018) (Fig. 1). Mean annual air temperatures in the region are ~29-30 °C (Fig. 2A) and mean annual lake water temperatures are on average, cooler by 1-2 °C (Harbott et al., 1982), although, lake temperatures may ephemerally rise in some months to as high as ~30-31 °C (Källqvist et al., 1988). There is a modest north-south temperature gradient, with surface waters being on average ~1 °C cooler (Harbott et al., 1982) towards the southern end of the lake (which is also deeper). The water column across the lake is generally well-mixed, although a seasonal thermocline and partial stratification may occur during certain times of the year (Källqvist et al., 1988).

Compared to adjacent regions, year-to-year variability in temperature and precipitation in Lake Turkana is relatively muted (Fig. 2). Interannual (year-to-year) variability, defined here as one standard deviation (1σ) of annual mean air temperatures is ~0.6-0.8°C (Fig. 2B; (Willmott & Matsuura, 2001)). Available measurements also indicate low seasonal and interannual variability of lake water temperatures (Harbott et al., 1982; Källqvist et al., 1988; Halfman, 1996). Interannual precipitation variability directly over the lake is below 15 cm/year (Fig. 2B) and exerts a negligible influence on the water mass and stable isotopic budget of Lake Turkana (Ricketts & Johnson, 1996). The Ethiopian highlands and the Omo-Gibe drainage regions encounter much stronger variability in rainfall (Fig. 2D), where rainwater isotope measurements also exhibit large (4-5 ‰, VSMOW) interannual variance (Bedaso et al., 2020).

Being the dominant influx to Lake Turkana, Omo River discharge modulates hydrological and geochemical variability in Lake Turkana (Ng'ang'a et al., 1998; Avery & Tebbs, 2018; Ricketts & Johnson, 1996). The rate of Omo River inflow and its geochemical composition influences the mean composition of Lake Turkana, as well as that of carbonates forming from lake waters (Ricketts & Anderson, 1998). Here, the $\delta^{18}O$ of authigenic and biogenic calcite – if precipitated in isotopic equilibrium – reflects the $\delta^{18}O_w$ and the temperature of the water mass at the time of formation (Halfman & Johnson, 1988; Johnson et al., 1991; Ricketts & Anderson, 1998). As temperature variability in the region is relatively minor, $\delta^{18}O_w$ has been shown to be the main control on the $\delta^{18}O$ of calcite (Ricketts & Johnson, 1996; Ricketts & Anderson, 1998). $\delta^{18}O_w$ in Lake Turkana is driven by the interplay between 1) the volume of net riverine flows into Lake Turkana (dominated by the Omo River), 2) the $\delta^{18}O$ composition of net inflows, and 3) the rate of evaporation over the lake (Johnson et al., 1991; Ricketts & Johnson, 1996; Ng'ang'a et al., 1998). Precipitation above the lake as well as its $\delta^{18}O$ composition negligibly affect the mean composition of Lake Turkana (Ricketts & Johnson, 1996). Omo River waters also bring in nutrients in the form of dissolved inorganic carbon (DIC), phosphate, and nitrate into Lake Turkana, and mediate carbon cycling in the lake (Johnson et al., 1991). Accordingly, the $\delta^{13}C$ of DIC in Omo River waters exerts an influence on the $\delta^{13}C$ of

calcite precipitated in Lake Turkana (Johnson et al., 1991). Available measurements of productivity in the lake generally delineate a latitudinal trend of decreasing primary production moving away from the northern plume (Government of Kenya and the Ministry of Overseas Development, 1982), additionally establishing the impact of Omo River inflow on Lake Turkana biogeochemistry.

Omo-Turkana sediments have been the focus of extensive geochemical study to investigate East African climate change across the Neogene. Geochemical records have been developed from stable isotopes in authigenic carbonates (Halfman & Johnson, 1988; Ricketts & Anderson, 1998; Johnson et al., 1991), biogenic carbonates including ostracodes (Halfman et al., 1989; Beck et al., 2019a; Beck et al., 2021; Ng'ang'a et al., 1998) mollusks (Abell, 1982; Forman et al., 2014; van der Lubbe et al., 2017; Vonhof et al., 2013) and stromatolites (Abell et al., 1982), pedogenic carbonates (Cerling et al., 1988; Levin, 2015; Beck et al., 2019b; Wynn, 2004; Quinn & Lepre, 2020), fossil teeth (Cerling et al., 2015; Cerling et al., 2011a), and using organic biomarkers (Uno et al., 2016; Lupien et al., 2018; Lupien et al., 2020; Morrissey & Scholz, 2014; Morrissey et al., 2018). Compared to the extensive studies characterizing modern stable isotope variability in authigenic (Ricketts & Anderson, 1998; Johnson et al., 1991; Halfman & Johnson, 1988; Halfman et al., 1994; Halfman et al., 1989), molluscan (Vonhof et al., 2013; Abell, 1982; van der Lubbe et al., 2017; Manobianco, 2021), and pedogenic carbonates (Cerling et al., 1988; Cerling et al., 2011b; Quinn & Lepre, 2020), to our knowledge, only three studies have investigated multi-specimen analyses of $\delta^{18}O$ and $\delta^{13}C$ for modern ostracodes from Lake Turkana (Ng'ang'a et al., 1998; Halfman et al., 1989), with only 35 previously published values on modern *S. clavularis*. In this work, we provide 329 new IOVA-$\delta^{13}C$ and -$\delta^{18}O$ measurements on individual *S. clavularis* specimens in modern sediments collected from Lake Turkana in 1979 and examine seasonal and climatic controls on their intra- and inter-site variance.

3. Materials and Methods

3.1. Sediment Samples and Stable Isotope Analysis

We use surface sediment samples to investigate modern ostracode geochemistry in Lake Turkana. Seventeen sediment samples were used in this study, which were collected across Lake Turkana in July-November 1979, using a modified Ekman dredge with a surface collection area of 225 cm^2 (samples taken from uppermost, biologically active zone-oxidized sediments). At certain sites, surface and bottom water temperatures were recorded; details about sampling methodologies have been reported previously (Cohen, 1984; Cohen, 1986). We note that these samples contained live organisms at the time of collection and that epifauna were isolated from infauna in undisturbed dredge samples (Cohen, 1986), thereby attesting to the modern age of these sediments. Individual calcitic valves of ostracode species *Sclerocypris cf. clavularis* (Cohen, 1986) were identified and picked from the >125 μm size fraction at each site (see Table 1 for details). Due to the rapid calcification of ostracode calcite (Turpen & Angell, 1971; Chivas et al., 1986; Roca & Wansard, 1997) and the lack of data implicating a seasonal preference for this species (Cohen, 1986), we assume that most of these valves calcified in the year prior to collection. Although we cannot rule out that these valves did not calcify over several years preceding 1979, sedimentation rates and the intactness of sample fauna suggest that they were not older than a year to a few years at the time of collection (Cohen, 1986).

We measured the mass and length (L1) and height (L2) of each valve using a Sartorius Cubis II Ultra-Micro Balance (precision = 0.5 µg) and a MeijiTechno HDZ7000TS Digital Zoom Microscope System (precision = 10 µm) respectively, housed at the Paleo^2 Laboratory at the University of Arizona. Owing to their relatively large masses (average mass of all valves was ~225 µg), valves were then gently cracked using a pin and fragments amounting to 20-80 µg were collected for stable isotopic analysis. IOVA-$\delta^{13}C$ and -$\delta^{18}O$ (n=329) - with values reported in permil (‰) relative to Vienna Pee Dee Belemnite (VPDB) – were measured using a Kiel IV Carbonate Device coupled to a MAT 253+ isotope ratio mass spectrometer housed at the Paleo^2 Laboratory at the University of Arizona. IAEA-603 standards (n=60) were used to monitor precision over the period of analyses and the reported statistics ($\delta^{13}C$ = 2.46 ± 0.03 ‰.; $\delta^{18}O$ = -2.37 ± 0.05 ‰) are consistent with the long-term precision of this setup (0.03 ‰ and 0.05 ‰ 1σ for $\delta^{13}C$ and $\delta^{18}O$ respectively). Intra-valve isotope heterogeneity was confirmed to be negligible as replicate analyses of fragments from an individual valve (n=23) were found to be identical to each other within analytical uncertainty.

3.2. $\delta^{18}O$ Equilibrium Considerations

To investigate oxygen isotope equilibrium, we used the experimentally determined equation provided by Kim & O'Neil, 1997:

$$1000ln\alpha_{calcite-water} = 18.03 * \left(\frac{10^3}{T}\right) - 32.42 \quad (1)$$

where T is temperature of calcite formation and α is the $^{18}O/^{16}O$ fractionation factor between calcite and water; note that $1000ln\alpha_{calcite-water} \approx \delta^{18}O_{calcite} - \delta^{18}O_{water}$. In tandem with the collected temperature data, the measured $\delta^{18}O$ of ostracode valve calcite (after conversion from VPDB to VSMOW) was used to calculate $\delta^{18}O_w$ and compared with measurements of $\delta^{18}O_w$ across different years of collection (Cerling et al., 1988; Cerling, 1996; Ricketts & Johnson, 1996).

As comprehensive measurements of organic carbon production, carbonate system parameters including alkalinity, DIC, and DIC-$\delta^{13}C$, and nutrient loading data in the Omo River or across Lake Turkana are not available, we refrain from assessing carbon isotope equilibrium constraints using our IOVA-$\delta^{13}C$ measurements.

3.3. Influence of Omo River Inflow and Related Statistical Analysis

We examined the relative influence of Omo River inflow on our geochemical measurements by calculating a north-to-south distance for each of our sites from a fixed arbitrary marker in the Omo River delta region (Fig. 1B), slightly north of Lake Turkana. Because the sharp bend in the lake precludes making a simple linear measurement from the marker point to the four sites in the southern part of the lake (Sites 79-189F, 79-193F, 79-204F, 79-194F), we added the distance of the initial marker to a fixed point in the central part of the lake (east of Site 79-183F) to their relative distances from that point. By assigning a distance (km) from Omo River inflow to each site, we were able to investigate proximity to the Omo River as a control on our measurements. We then applied weighted linear regression using maximum likelihood estimation to calculate the Pearson correlation coefficient and line of best fit (York et al., 2004; Thirumalai et al., 2011). Whereas analytical precision (1σ) was used as error-based weights for the regression across all isotope data (Fig. 3), we used the intra-site standard deviation ($1\sigma_{intra}$) between individual valves as weights for the inter-site regressions (Figs. 4-5; including for regressions with mass, L1, and L2 – see Table 2). Finally, we compared the calculated $\delta^{18}O_w$ at

each site (assumed as a baseline for 1979) with direct measurements of $\delta^{18}O_w$ collected in January 1994 (Ricketts & Johnson, 1996) (see Fig. 5). Errors for the inversion of $\delta^{18}O_w$ were propagated using a Monte Carlo procedure (n=1000 for each site), where mean values were allowed to normally vary about the root mean square error calculated using both analytical uncertainty and $1\sigma_{intra}$ at each site (Table 1).

4. Results

4.1. Negligible Influence of Valve Morphometrics on Stable Isotopes

Pooled statistics (mean and standard deviation) of stable isotopes, mass, valve length (L1), and height (L2) with an average number of ~19 valves analyzed per site, are presented in Table 1. We calculated inter-site correlation coefficients for each of these parameters using the pooled data at each site (Table 2). The average mass, length, and height across all ostracode valves was 225 (±50) µg, 2.09 (±0.11) mm, and 1.09 (± 0.07) mm. We found no significant correlations between stable isotope composition (either $\delta^{13}C$ or $\delta^{18}O$) and valve mass, height, or length across all samples ($p > 1$ & $r^2 < 0.02$ across each combination; not shown), or when comparing mean values across each site (Table 2). Owing to significant correlations only amongst other morphometric variables and lack of covariance with stable isotopes, latitude, longitude, depth, and distance (Table 2), we conclude that the *S. clavularis* morphometrics (valve mass, length, and height) do not have a discernable environmental sensitivity nor do they impact the stable isotopic composition of their valve material.

4.2. Inter-site Covariance of Modern *S. clavularis* $\delta^{13}C$ and $\delta^{18}O$ at Lake Turkana

Stable carbon and oxygen isotopes in modern *S. clavularis* at Lake Turkana exhibit a range of ~6 ‰ ($\delta^{13}C_{max}$ = 0.87 ‰; $\delta^{13}C_{min}$ = -5.14 ‰) and ~3.8 ‰ ($\delta^{18}O_{max}$ = 5.37 ‰; $\delta^{18}O_{min}$ = 1.59 ‰) relative to VPDB, respectively, across all measured samples (Fig. 3). As is expected for closed-basin lakes (Talbot, 1990), we observe a significant positive correlation between $\delta^{13}C$ and $\delta^{18}O$ ($p<0.001$; $r = 0.54$) of ostracode calcite, with the line of best-fit being:

$$\delta^{13}C = -10.38\ (\pm 0.10) + 2.54\ (\pm 0.03) * \delta^{18}O \qquad (2)$$

The range of these values encompasses all previous (albeit multi-specimen and not IOVA) measurements of modern *S. clavularis* $\delta^{18}O$ and $\delta^{13}C$ from Lake Turkana sediments (Ng'ang'a et al., 1998; Halfman et al., 1989). Ng'ang'a and colleagues (1998) found that the average of modern *Hemicypris intermedia* $\delta^{13}C$ and $\delta^{18}O$ (squares in Fig. 3A) was consistently higher than that of *S. clavularis* (circles in Fig. 3A) in Lake Turkana – further confirmed by Beck et al. (2021). Compared to our newly generated *S. clavularis* data (Fig. 3A), collectively, the previously published measurements of *H. intermedia* indeed cluster towards the most positive $\delta^{13}C$ *S. clavularis* values, although $\delta^{18}O$ values ranged within our *S. clavularis* measurements (Fig. 3A). Similarly, $\delta^{18}O$ of modern specimens of *Potamocypris worthingtoni* were within range of all available *S. clavularis* $\delta^{18}O$, although $\delta^{13}C$ was systematically higher (Fig. 3A triangles). This could be related to the fact that most of the multi-specimen measurements presented in Beck et al. (2021) were sampled from shallow regions of the lake (~3-5 m) or from beaches. However, *P. worthingtoni* is also known to be a shallow water dweller, which could additionally explain the higher $\delta^{13}C$ values of this species (Cohen, 1986). The average *S. clavularis* $\delta^{13}C$ and $\delta^{18}O$ values in our study (n=329) were -1.71 and 3.38 ‰. We note that the average $\delta^{13}C$ (-2.08

269 ‰; n = 35) and $\delta^{18}O$ (3.13 ‰; n = 35) in previous studies (Ng'ang'a et al., 1998; Halfman et al.,
270 1989) are offset relative to our samples by ~0.2 ‰ and ~0.3 ‰ respectively, which may be
271 related to more limited spatial sampling. Overall, previous multi-specimen *S. clavularis* $\delta^{13}C$ and
272 $\delta^{18}O$ are consistent with the range of our IOVA measurements.

273 When we pool our *S. clavularis* measurements by location (n=17; Fig. 3B), the range of
274 mean IOVA values spans 2.27 ‰ (VPDB) in $\delta^{13}C$ and 2.01 ‰ (VPDB) in $\delta^{18}O$ across the sites,
275 with lower values in the northern part of the lake. The positive correlation between site-based
276 mean IOVA-$\delta^{13}C$ and -$\delta^{18}O$ becomes stronger ($p<0.001$; $r = 0.75$) relative to the regression
277 containing all measured samples (Fig. 3A-B). The inter-site pooled means exhibit a line of best-
278 fit having an intercept closer to zero and a lower $\delta^{13}C$-$\delta^{18}O$ slope than that constructed with all
279 measurements, albeit with higher uncertainty due to the incorporation of within-site variability
280 ($1\sigma_{intra}$) as errors (Fig. 3b):

281 $$\delta^{13}C = -5.21\ (\pm 1.73) + 1.02\ (\pm 0.51) * \delta^{18}O \qquad (3)$$

282 Mean IOVA-$\delta^{13}C$ and -$\delta^{18}O$ values across the sites show significant correlations (Table 2)
283 with depth (both $\delta^{13}C$ and $\delta^{18}O$), latitude (both $\delta^{13}C$ and $\delta^{18}O$), and longitude (only $\delta^{18}O$).
284 However, we find that the omission of the four southernmost sites bring about reductions in
285 covariance with depth (r^2 reduces from 0.78 to 0.46 for $\delta^{18}O$, and from 0.32 to 0.31 for $\delta^{13}C$) and
286 longitude (r^2 reduces from 0.46 to 0 for $\delta^{18}O$ and remains unchanged at 0.06 for $\delta^{13}C$). It is worth
287 noting that the southern basin veers towards the east and is notably deeper than the north such
288 that correlations with longitude are driven by the shape of the lake. Nevertheless, correlations
289 with latitude remain high with ($r^2 = 0.55$ for $\delta^{18}O$; $r^2 = 0.31$ for $\delta^{13}C$) or without omission ($r^2 =$
290 0.78 for $\delta^{18}O$; $r^2 = 0.32$ for $\delta^{13}C$) of the four southern sites.

291 **4.3. Similar Intra-Site Stable Isotopic Variance Across Lake Turkana Sites**

292 At all sites we find larger IOVA-$\delta^{13}C$ variance than that of IOVA-$\delta^{18}O$ (Table 1). $\delta^{18}O$
293 variability at each site (*i.e.*, $1\sigma_{intra}$) ranges from 0.28 ‰ (Site 79-166F) to 0.57 ‰ (Site 79-193F),
294 whereas inter-site $\delta^{13}C$ variability ranges from 0.68 ‰ (Site 79-166F) to 1.32 ‰ (Site 79-183F).
295 Additionally, we note that these two parameters themselves are not significantly correlated
296 across sites (Table 2), nor are they correlated with water depth, longitude, latitude, or distance
297 from Omo River inflow. Average IOVA-$\delta^{13}C$ and -$\delta^{18}O$ $1\sigma_{intra}$ across all sites combined is 1.00
298 (±0.21) ‰ and 0.42 (±0.10) ‰, indicating that the mean $1\sigma_{intra}$ is larger than site-to-site stable
299 isotope variance. This observation is consistent with the inference that ostracode valve
300 calcification across the entire lake encounters similar carbon and oxygen isotope variability,
301 despite different inter-site mean values.

302 **4.4. Near-Equilibrium Oxygen Isotope Calcification of *S. clavularis***

303 We compiled available measurements of modern $\delta^{18}O_w$ at Lake Turkana (Cerling, 1996;
304 Cerling et al., 1988; Ricketts & Anderson, 1998) alongside our ostracode $\delta^{18}O$ and *in situ* bottom
305 water temperature measurements (Cohen, 1981; Cohen, 1984) to determine whether ostracode
306 calcification took place under isotopic equilibrium. In total, we compiled thirty seven published
307 $\delta^{18}O_w$ values whose average $\delta^{18}O$ is 5.72 ± 0.71 (1σ) ‰ (reported relative to VSMOW) collected
308 from the lake across different years, comprised of three samples collected in September 1975,

March 1977, and August 1980 (Cerling et al., 1988) (locations unknown; average ä$^{18}O_w$ = 5.83 ‰), 17 samples collected between September 1980 and September 1982 (average $\delta^{18}O_w$ = 6.1 ‰) at the Koobi Fora spit (Cerling, 1996) located south of our sampling site BS-91 on the eastern flank of the lake (Fig. 2), and 17 samples collected across various sites along the lake (Ricketts & Johnson, 1996) in January 1994 (average $\delta^{18}O_w$ = 5.48 ‰). $\delta^{18}O_w$ data from Ricketts and Johnson (1996) clearly delineate a north-to-south trend towards ^{18}O enrichment away from the Omo River inflow (green points in Fig. 5A) and confirm the importance of changing $\delta^{18}O_w$ as a contributor of calcite $\delta^{18}O$ precipitation across the lake. Thus, to minimize biases associated with ephemeral spatiotemporal $\delta^{18}O_w$ sampling across the lake and to maximize available measurements, we focus on a sub-selection of *in situ* temperature, IOVA-$\delta^{18}O$, and $\delta^{18}O_w$ samples collected north of the Koobi Fora spit to assess isotopic equilibrium.

The average $\delta^{18}O_w$ of available samples (n_{sites} = 2; n_{total} = 19) across the northern portion (>3.9°N) of Lake Turkana is 5.86 ± 0.56 (1σ) ‰ (VSMOW) which, coupled with average *S. clavularis* $\delta^{18}O$ of 2.98 ± 0.28 (1σ) ‰ (VPDB; n_{sites} = 6; n_{total} = 105) in this domain yields an average calcification temperature of 25.3 ± 2.8 °C (1σ propagated error) using equation (1); this estimate is virtually identical to average *in situ* bottom water measurements (n_{sites} = 4; n_{total} = 4) of 25.3 ± 1.5 (1σ) °C (Table 3). We note that even this sub-selection of samples may not be an appropriate "apples to apples" comparison for equilibrium constraints as coevally collected ostracodes, bottom water temperature, and $\delta^{18}O_w$ data do not exist. If we focus solely on IOVA-$\delta^{18}O$ measurements at BS-90 and BS-91 (average $\delta^{18}O$ = 3.11 ± 0.5 ‰; n_{total} = 34), proximal to the Koobi Fora spit, and apply the nearest *in situ* bottom-water temperature (23.5 °C at site 79-168F; 36 km away), we obtain a $\delta^{18}O_w$ estimate of 5.73 ± 0.51 (1σ propagated error) ‰ (VSMOW; see Table 3). This reconstructed value is identical within uncertainty to the average $\delta^{18}O_w$ of 5.74 ± 0.57 (1σ) ‰ (VSMOW), measured at that location (n_{total} = 17), although we further caution that the Koobi Fora water samples were collected long after our 1979 sample collection (Cerling, 1996). Assuming that the average bottom-water temperature of calcification for ostracodes across the entire lake to be 25.7°C (the average of our *in situ* bottom water measurements), the average IOVA-$\delta^{18}O$ of all our measurements (3.40 ‰; n = 352) points to a mean Turkana $\delta^{18}O_w$ value of 6.4 ± 0.5 ‰ for 1979 (*i.e.,* over the average duration of calcification of ostracode valves in our sample), which is within the range of $\delta^{18}O_w$ (4.75 - 8.95 ‰) measured in subsequent years. Finally, we note that if we pool all available $\delta^{18}O_w$ measurements (n=17) along with all ostracode $\delta^{18}O$ measurements (n=329), we obtain a mean bottom-water temperature estimate of 22.5 °C with a propagated uncertainty of ±3.8 °C (Table 3). Although within uncertainty, this median estimate is cooler than most available measurements (Harbott et al., 1982; Cohen, 1986; Källqvist et al., 1988) and suggests that inaccuracies may arise due to the lack of *in situ* bottom water $\delta^{18}O_w$ measurements paired with ostracode calcite $\delta^{18}O$.

Overall, our data are consistent with the average $\delta^{18}O$ of numerous individual valves being deposited at apparent (or near) equilibrium conditions. Considering sampling uncertainty in the other parameters, we cannot rule out small deviations from equilibrium on the order of ~0.2-0.3 ‰ (VPDB). That said, our analysis rules out that *S. clavularis* $\delta^{18}O$ deviates from equilibrium by 0.5-1.5 ‰, as hypothesized previously (Ng'ang'a et al., 1998) using a much smaller number of samples (Fig. 3). Although future coeval sampling may provide more precise

insights, we conclude that IOVA-$\delta^{18}O$ measurements in tandem with available environmental data are consistent with calcification close to oxygen isotope equilibrium.

4.5. Large Intra-Site and Inter-Site IOVA-$\delta^{13}C$ Variability

IOVA-$\delta^{13}C$ across Lake Turkana samples range from 0.87 ‰ to -5.14 ‰ (~6‰), exhibiting large intra-site variability (average intra-site $1\sigma = 1 \pm 0.21$ ‰; Table 1), with an average value of -1.75 ‰. The average intra-site standard deviation of IOVA-$\delta^{13}C$ values is more than double of its IOVA-$\delta^{18}O$ counterpart, and points towards more complex controls. Amongst other factors, ostracode $\delta^{13}C$ is influenced by DIC-$\delta^{13}C$ values in waters where they calcify (Xia et al., 1997; Pérez et al., 2013), which can be driven by ^{13}C enrichment due to primary productivity (Källqvist et al., 1988) or due to varying riverine $\delta^{13}C$ inputs. However, dietary preferences can also alter ostracode $\delta^{13}C$ (Limén & Ólafsson, 2002) – a process which may be particularly relevant to *S. clavularis*, which feeds on organic detritus (Cohen, 1986). Whereas higher surface production and organic matter consumption lead to lower benthic $\delta^{13}C$ (Källqvist et al., 1988; Pérez et al., 2013), out-of-phase seasonal stratification and Omo River inflow(Källqvist et al., 1988), could explain the large variance in IOVA-$\delta^{13}C$. Nevertheless, mean IOVA-$\delta^{13}C$ across sites yield a significant slope of 0.1 ‰ (VPDB) per 10 km that mirrors the $\delta^{18}O$ slope (Fig. 4), despite higher uncertainty owing to high $1\sigma_{intra}$ for $\delta^{13}C$ between valves. This observation points to the Omo River influx as the main driver of the spatial patterns of both IOVA-$\delta^{18}O$ and $\delta^{13}C$ across our sites.

5. Discussion

Our IOVA datasets reveal a strong imprint of Omo River inflow on Lake Turkana geochemistry. The observed latitudinal trends across mean IOVA values arises due to the north-south geometry of the lake basin and the southward dissipation of the Omo River plume into the lake (Fig. 4). Accordingly, we find that using distance from Omo River inflow as a predictor yields the strongest correlations with mean IOVA-$\delta^{13}C$ ($r^2 = 0.33$) and $\delta^{18}O$ ($r^2 = 0.81$) values (Table 2). Considering near-equilibrium calcification for $\delta^{18}O$ (see Section 4.4) and assuming the same for $\delta^{13}C$, inter-site IOVA means exhibit more enriched ^{18}O and ^{13}C of ostracode calcite towards the southern part of the lake and support that low-$\delta^{18}O$/$\delta^{13}C$ Omo River waters (Cerling et al., 1988) modulate mean stable isotopic variability across Lake Turkana.

Superimposed on the southward waning of the low-$\delta^{18}O$ Omo River plume, ^{18}O enrichment in ostracode calcite is linked to evaporation over the lake (green dots in Fig. 5A), which additionally serves to heighten $\delta^{18}O_w$ (Cerling et al., 1988; Cerling, 1996; Johnson et al., 1991; Ricketts & Johnson, 1996). Assuming a mean temperature of calcification (25.7°C) based on all available bottom water temperature measurements from 1979 (and applying a 1°C north-south difference to the four southern-most sites), we calculated $\delta^{18}O_w$ from our inter-site IOVA-$\delta^{18}O$ dataset (orange points in Fig. 5A). This yields a reconstructed $\delta^{18}O_w$ range of ~1.8 ‰ (VSMOW), which is similar to the range measured by Ricketts and Johnson (1996) across the lake in January 1994 (~1.31 ‰); we note that their sampling range did not extend as far south as ours, and if we limit our samples to their same range (based on distance from Omo River inflow), our reconstructed $\delta^{18}O_w$ range becomes ~1.2 ‰ (*i.e.,* omitting the northernmost and southernmost values; see Fig. 5). Despite similar ranges and slopes however, the reconstructed inter-site $\delta^{18}O_w$ for samples collected in 1979 are offset, on average, by 0.9 ‰ relative to

measurements in January 1994 (Fig. 5A). As the Omo River is ultimately sourced from precipitation in the Ethiopian highlands, for illustrative purposes, we investigated mean annual precipitation anomalies between 1979 and 1993 (*i.e.*, the year preceding January 1994; Fig. 5B) as a cause for the $\delta^{18}O_w$ offset using monthly GPCC station-based rainfall data (Beck et al., 2005). Interestingly, we find that the northern portion of the Omo catchment received far more precipitation (>20 cm) in 1993 relative to 1979 whereas surrounding catchments of other rivers that do not drain into Turkana were anomalously dry (Fig. 5B). Thus, increased rainfall in the Ethiopian highlands during 1993 relative to 1979 could explain the offset in $\delta^{18}O_w$ between the years – either via increased volume of Omo River discharge or via more negative $\delta^{18}O$ of Omo River waters fed by more negative $\delta^{18}O$ of precipitation (Ricketts & Anderson, 1998). We caution that this exercise unrealistically simplifies several hydrometeorological complexities of $\delta^{18}O$ fractionation including processes related to seasonality, clouds, spatial variability in riverine discharge, catchment storage etc. (Bedaso et al., 2020; Dasgupta et al., 2021; Maupin et al., 2021). Nevertheless, it provides confidence in using IOVA-$\delta^{18}O$ to reconstruct lake water $\delta^{18}O_w$ and its links with rainfall from where the Omo River is sourced. Future research may refine the quantitative relationship between Ethiopian rainfall $\delta^{18}O$, Omo River discharge, and IOVA-reconstructed lake water $\delta^{18}O_w$. Overall, our data are consistent with higher precipitation in the Omo catchment leading to lowered Lake Turkana $\delta^{18}O_w$, as proposed before (Halfman & Johnson, 1988; Johnson et al., 1991; Ricketts & Johnson, 1996).

Whereas few carbonate system measurements exist to sufficiently investigate controls on ostracode $\delta^{13}C$ across Lake Turkana, co-variance between inter-site mean IOVA-$\delta^{13}C$ with distance from inflow (Fig. 4B) suggest an Omo River control. We suggest that such a trend towards positive $\delta^{13}C$ values towards the southern part of the lake could arise due to two possible effects: 1) dilution of low-$\delta^{13}C$ values of the Omo River plume (Johnson et al., 1991), and 2) dilution of nutrients associated with the riverine plume leading to lower primary production (Government of Kenya and the Ministry of Overseas Development, 1982; Källqvist et al., 1988) and hence, higher DIC-$\delta^{13}C$ in bottom waters towards the southern part of the lake owing to lower amounts of microbially mediated breakdown of organic matter. Although no direct measurements of DIC-$\delta^{13}C$ exist for the Omo River, its $\delta^{13}C$ likely falls between -5 to -15 ‰ in accordance with other East African river waters (Cerling et al., 1988; Johnson et al., 1991) – far more negative than measured lake water DIC-$\delta^{13}C$, which range between 0 and -1 ‰ at the Koobi Fora spit (Cerling, 1996). Production in Turkana is N-limited (Källqvist et al., 1988), and Omo River inflow brings large amounts of nitrates into the lake that cause blooms towards the north (Källqvist et al., 1988; Avery & Tebbs, 2018). Here, it may be likely that organic matter $\delta^{13}C$ is highly negative due to large photosynthetic fractionation (Hodell & Schelske, 1998), and microbial breakdown of organic matter would result in low-$\delta^{13}C$ bottom water DIC, which imprints itself onto benthic ostracode calcite (Pérez et al., 2013). Moreover, considering that *S. clavularis* is a detritivore feeding on deposited particulate organic matter (Cohen, 1986), the carbon isotopic composition of its diet could imprint its $\delta^{13}C$ on the ostracode valve during calcification (*i.e.*, a "vital effect"). Both dilution effects are consistent with our observation of higher mean IOVA-$\delta^{13}C$ towards the southern part of the lake. Complex interactions between these effects could confound straightforward interpretations of IOVA-$\delta^{13}C$ and may in part explain the high variance we observe. As one example, wind-driven mixing during seasons outside that of riverine pulses could regenerate nutrients in surface waters from the deep and promote primary production. Thus, we recommend caution in downcore interpretations of IOVA-$\delta^{13}C$ linked solely to primary production. Taken together, the mean IOVA-$\delta^{13}C$ and $1\sigma_{intra}$

of our measurements (2.11 ± 0.1 ‰, VPDB) provide a modern reference for future IOVA-$\delta^{13}C$ applications.

Overall, our results suggest that pooled averages of IOVA measurements can accurately reflect mean limnological conditions in Lake Turkana, and hence IOVA may be an effective tool to infer paleotemperature and paleohydrology in the region. However, site-based IOVA values also capture the large spatial variability across the lake, on the order of several permille in both IOVA-$\delta^{18}O$ and -$\delta^{13}C$ (Fig. 4). As this basin is thought to have encountered large lake-level changes over the Holocene and Pleistocene – changes that may have decoupled the northern and southern parts of the basin (Bloszies et al., 2015) – we suggest that downcore investigations of IOVA at Lake Turkana and related inferences about paleohydrology be conducted with this spatial dimension in mind, in addition to analyzing large numbers of valves.

Can IOVA-$\delta^{18}O$ be used to reconstruct interannual hydroclimate variability or its seasonality? The average $1\sigma_{intra}$ for ostracode $\delta^{18}O$ measurements across all sites is 0.42 ± 0.10 ($1\sigma_{\sigma\text{-}intra}$) ‰ (VPDB; Table 1). The average year-to-year (1σ) temperature variability across the lake is ~0.45 °C (Fig. 2B), and the standard deviation of climatological seasonal cycle of temperature is ~0.7 °C (not shown). If we assume that these parameters are accurate for bottom water temperatures (which is likely an overestimate), this could explain up to ~0.18 ‰ (VPDB) of the average $1\sigma_{intra}$ values, using a slope of 0.22 ‰/°C and the root mean square estimate for combining both forms of variability (Kim & O'Neil, 1997). Thus, the remaining ~0.24 ‰, amounting to ~60% of the average IOVA-$\delta^{18}O$ $1\sigma_{intra}$, must arise from processes related to $\delta^{18}O_w$ and hydroclimate changes. Our attribution of temperature versus hydroclimatic variability is probably an underestimate as our samples are not likely to record multiple years of data to capture the full range of interannual variability (see Materials and Methods). We suggest that IOVA-$\delta^{18}O$ applied to downcore sediments may be compared to our modern baseline value of variability (0.42 ± 0.10 ‰) to examine whether seasonality or interannual variability of temperature and hydroclimate at Lake Turkana was altered during past periods.

6. Conclusions

We propose that with enough analyses to overcome inter-specimen isotopic variance (n>~20), IOVA of *S. clavularis* in Lake Turkana sediments can be a highly skillful indicator of mean limnological and hydrological conditions and variability in the region. IOVA-$\delta^{18}O$ measurements (n=392) from various sites across the lake match well with available *in situ* observations of bottom water temperature ($\delta^{18}O_w$) and are consistent with being deposited under near-equilibrium conditions. Average IOVA-$\delta^{13}C$ and -$\delta^{18}O$ are highly correlated with each other (Fig. 3), and with proximity to Omo River inflow (Fig. 4), revealing a dominant river-plume influence on Lake Turkana biogeochemistry. We conclude that IOVA performed at Lake Turkana can accurately reflect the hydrological history of Omo River source-waters in the Ethiopian highlands.

Acknowledgements

We thank Thure Cerling, Tom Johnson, and Doug Ricketts for providing water chemistry data from Lake Turkana, and Lael Vetter for assistance in ostracode morphometric data collection. KT thanks the University of Arizona Technology and Research Initiative Fund

(TRIF). All data from this study are available in the supplementary section and are in the process of being uploaded to an appropriate online data repository.

References

Abell, P. I. (1982). Palaeoclimates at Lake Turkana, Kenya, from oxygen isotope ratios of gastropod shells. *Nature*, *297*(5864), 321-323. https://www.nature.com/articles/297321a0

Abell, P. I., Awramik, S. M., Osborne, R. H., & Tomellini, S. (1982). Plio-Pleistocene lacustrine stromatolites from Lake Turkana, Kenya: morphology, stratigraphy and stable isotopes. *Sedimentary Geology*, *32*(1-2), 1-26. http://citeseerx.ist.psu.edu/viewdoc/download?doi=10.1.1.710.2024&rep=rep1&type=pdf

Avery, S. T., & Tebbs, E. J. (2018). Lake Turkana, major Omo River developments, associated hydrological cycle change and consequent lake physical and ecological change. *Journal of Great Lakes Research*, *44*(6), 1164-1182. https://doi.org/10.1016/j.jglr.2018.08.014

Beck, C., Grieser, J., & Rudolf, B. (2005). A new monthly precipitation climatology for the global land areas for the period 1951 to 2000. *Geophysical Research Abstracts*, *7*(07154). http://www.juergen-grieser.de/publications/publications_pdf/Beck_Grieser_Rudolf_EGU_05.pdf

Beck, C. C., Feibel, C. S., Wright, J. D., & Mortlock, R. A. (2019a). Onset of the African humid period by 13.9 kyr BP at Kabua Gorge, Turkana Basin, Kenya. *The Holocene*, *29*(6), 1011-1019. https://journals.sagepub.com/doi/pdf/10.1177/0959683619831415

Beck, C. C., Allen, M. M., Feibel, C. S., Beverly, E. J., Stone, J. R., Wegter, B., & Wilson, C. L. (2019b). Living in a swampy paradise: Paleoenvironmental reconstruction of an African Humid Period lacustrine margin, West Turkana, Kenya. *Journal of African Earth Sciences*, *154*, 20-34. https://doi.org/10.1016/j.jafrearsci.2019.03.007

Beck, C. C., Feibel, C. S., Mortlock, R. A., Quinn, R. L., & Wright, J. D. (2021). Little Ice Age to modern lake-level fluctuations from Ferguson's Gulf, Lake Turkana, Kenya, based on sedimentology and ostracod assemblages. *Quaternary Research*, 1-14. https://doi.org/10.1017/qua.2020.105

Bedaso, Z. K., DeLuca, N. M., Levin, N. E., Zaitchik, B. F., Waugh, D. W., Wu, S.-Y., Harman, C. J., & Shanko, D. (2020). Spatial and temporal variation in the isotopic composition of Ethiopian precipitation. *Journal of Hydrology*, *585*, 124364. https://doi.org/10.1016/j.jhydrol.2019.124364

Bloszies, C., Forman, S. L., & Wright, D. K. (2015). Water level history for Lake Turkana, Kenya in the past 15,000years and a variable transition from the African Humid Period to Holocene aridity. *Global and Planetary Change*, *132*, 64-76. https://doi.org/10.1016/j.gloplacha.2015.06.006

Cerling, T. E., Andanje, S. A., Blumenthal, S. A., Brown, F. H., Chritz, K. L., Harris, J. M., Hart, J. A., Kirera, F. M., Kaleme, P., Leakey, L. N., Leakey, M. G., Levin, N. E., Manthi, F. K., Passey, B. H., & Uno, K. T. (2015). Dietary changes of large herbivores in the Turkana Basin, Kenya from 4 to 1 Ma. *Proc Natl Acad Sci U S A*, *112*(37), 11467-11472. https://doi.org/10.1073/pnas.1513075112

Cerling, T. E., Levin, N. E., & Passey, B. H. (2011a). Stable isotope ecology in the Omo-Turkana Basin. *Evol Anthropol*, *20*(6), 228-237. https://doi.org/10.1002/evan.20326

Cerling, T. E., Wynn, J. G., Andanje, S. A., Bird, M. I., Korir, D. K., Levin, N. E., Mace, W., Macharia, A. N., Quade, J., & Remien, C. H. (2011b). Woody cover and hominin

environments in the past 6 million years. *Nature*, *476*(7358), 51-56. https://doi.org/10.1038/nature10306

Cerling, T. E. (1996). Pore water chemistry of an alkaline rift valley lake: Lake Turkana, Kenya. In T. C. Johnson, Odada, EO (Ed.), *The Limnology, Climatology, and Paleoclimatology of the East African Lakes* (pp. 225-240). Univ. of Utah, Salt Lake City (USA).

Cerling, T. E., Bowman, J. R., & O'Neil, J. R. (1988). An isotopic study of a fluvial-lacustrine sequence: the Plio-Pleistocene Koobi Fora sequence, East Africa. *Palaeogeography, palaeoclimatology, palaeoecology*, *63*(4), 335-356. https://www.sciencedirect.com/science/article/pii/0031018288901046

Chivas, A. R., Deckker, P. D., & Shelley, J. M. G. (1986). Magnesium and strontium in non-marine ostracod shells as indicators of palaeosalinity and palaeotemperature. *Hydrobiologia*, *143*, 135-142. https://link.springer.com/chapter/10.1007/978-94-009-4047-5_20

Cohen, A. S. (1981). Paleolimnological research at Lake Turkana, Kenya. *Palaeoecology of Africa*, *13*(1981), 61-82.

Cohen, A. S. (1984). Effect of zoobenthic standing crop on laminae preservation in tropical lake sediment, Lake Turkana, East Africa. *Journal of Paleontology*, *58, No. 2, Trace Fossils and Paleoenvironments: Marine Carbonate, Marginal Marine Terrigenous and Continental Terrigenous Settings*(Mar., 1984), 499-510. https://doi.org/10.2307/1304798

Cohen, A. S. (1986). Distribution and faunal associations of benthic invertebrates at Lake Turkana, Kenya. *Hydrobiologia*, *141*(3), 179-197. https://link.springer.com/article/10.1007/BF00014214

Dasgupta, B., Ajay, A., Kumar, A., Thamban, M., & Sanyal, P. (2021). Isoscape of Surface Runoff in High Mountain Catchments: An Alternate Model for Meteoric Water Characterization and Its Implications. *Journal of Geophysical Research: Atmospheres*, *126*(16). https://doi.org/10.1029/2020jd033950

Dettman, D. L., Smith, A. J., Rea, D. K., Moore Jr, T. C., & Lohmann, K. C. (1995). Glacial meltwater in Lake Huron during early postglacial time as inferred from single-valve analysis of oxygen isotopes in ostracodes. *Quaternary Research*, *43*(3), 297-310. http://scholar.google.com/scholar?output=instlink&nossl=1&q=info:t4iweW9qlHEJ:scholar.google.com/&hl=en&as_sdt=0,3&scillfp=3085559159630797961&oi=lle

Dettman, D. L., Palacios-Fest, M. R., Nkotagu, H. H., & Cohen, A. S. (2005). Paleolimnological investigations of anthropogenic environmental change in Lake Tanganyika: VII. Carbonate isotope geochemistry as a record of riverine runoff. *Journal of Paleolimnology*, *34*(1), 93-105. https://doi.org/10.1007/s10933-005-2400-x

Dixit, Y., Hodell, D. A., Sinha, R., & Petrie, C. A. (2014). Abrupt weakening of the Indian summer monsoon at 8.2 kyr B.P. *Earth and Planetary Science Letters*, *391*, 16-23. https://doi.org/10.1016/j.epsl.2014.01.026

Dixit, Y., Hodell, D. A., Sinha, R., & Petrie, C. A. (2015). Oxygen isotope analysis of multiple, single ostracod valves as a proxy for combined variability in seasonal temperature and lake water oxygen isotopes. *Journal of Paleolimnology*, *53*(1), 35-45. https://doi.org/10.1007/s10933-014-9805-3

Escobar, J., Curtis, J. H., Brenner, M., Hodell, D. A., & Holmes, J. A. (2010). Isotope measurements of single ostracod valves and gastropod shells for climate reconstruction: evaluation of within-sample variability and determination of optimum sample size. *Journal of Paleolimnology*, *43*(4), 921-938. https://doi.org/10.1007/s10933-009-9377-9

573 Forman, S. L., Wright, D. K., & Bloszies, C. (2014). Variations in water level for Lake Turkana
574 in the past 8500 years near Mt. Porr, Kenya and the transition from the African Humid
575 Period to Holocene aridity. *Quaternary Science Reviews*, *97*, 84-101.
576 https://www.sciencedirect.com/science/article/pii/S0277379114001747
577 Government of Kenya and the Ministry of Overseas Development, L. (1982). Studies On Algal
578 Dynamics And Primary Productivity. In A. J. Hopson (Ed.), *Lake Turkana: A Report on the*
579 *Findings of the Lake Turkana Project 1972-1975* (Vol. 1, pp. 109-162). Institute of
580 Aquaculture, University of Stirling.
581 https://archive.org/details/laketurkanarepor1198hops/page/n5/mode/2up
582 Halfman, J. D. (1996). CTD-transmissometer profiles from Lakes Malawi and Turkana. *The*
583 *Limnology, Climatology and Paleoclimatology of the East African Lakes*, 169-182.
584 Halfman, J. D., & Johnson, T. C. (1988). High-resolution record of cyclic climatic change during
585 the past 4 ka from Lake Turkana, Kenya. *Geology*, *16*(6), 496-500.
586 https://pubs.geoscienceworld.org/geology/article-lookup/16/6/496
587 Halfman, J. D., Johnson, T. C., & Finney, B. P. (1994). New AMS dates, stratigraphic
588 correlations and decadal climatic cycles for the past 4 ka at Lake Turkana, Kenya.
589 *Palaeogeography, Palaeoclimatology, Palaeoecology*, *111*(1-2), 83-98.
590 https://www.sciencedirect.com/science/article/pii/0031018294903492
591 Halfman, J. D., Johnson, T. C., Showers, W. J., & Lister, G. S. (1989). Authigenic low-Mg
592 calcite in Lake Turkana, Kenya. *Journal of African Earth Sciences (and the Middle East)*,
593 *8*(2-4), 533-540. https://www.sciencedirect.com/science/article/pii/S0899536289800430
594 Harbott, B. J., Ferguson, A. J. D., & Hopson, A. J. (1982). *The Lake Turkana Fisheries*
595 *Research Project 1972-1975. A Summary Of The Findings*. In.
596 Heaton, T. H. E., Holmes, J. A., & Bridgwater, N. D. (1995). Carbon and oxygen isotope
597 variations among lacustrine ostracods: implications for palaeoclimatic studies. *The*
598 *Holocene*, *5*(4), 428-434.
599 https://journals.sagepub.com/doi/pdf/10.1177/095968369500500405
600 Hodell, D. A., & Schelske, C. L. (1998). Production, sedimentation, and isotopic composition of
601 organic matter in Lake Ontario. *Limnology and Oceanography*, *43*(2), 200-214.
602 https://aslopubs.onlinelibrary.wiley.com/doi/abs/10.4319/lo.1998.43.2.0200
603 Holmes, J. A., Street-Peffott, F. A., Ivanovich, M., & Peffott, R. A. (1995). A late Quaternary
604 palaeolimnological record from Jamaica based on trace-element chemistry of ostracod
605 shells. *Chemical Geology*, *124*(1-2), 143-160.
606 https://www.sciencedirect.com/science/article/pii/000925419500032H
607 Holmes, J. A. (2008). Sample-size implications of the trace-element variability of ostracod
608 shells. *Geochimica et Cosmochimica Acta*, *72*(12), 2934-2945.
609 https://doi.org/10.1016/j.gca.2008.03.020
610 Johnson, T. C., Halfman, J. D., & Showers, W. J. (1991). Paleoclimate of the past 4000 years at
611 Lake Turkana, Kenya, based on the isotopic composition of authigenic calcite.
612 *Palaeogeography, Palaeoclimatology, Palaeoecology*, *85*(3-4), 189-198.
613 https://www.sciencedirect.com/science/article/pii/003101829190158N
614 Källqvist, T., Lien, L., & Liti, D. (1988). Lake Turkana limnologlcal study 1985-1988.
615 *Norwegian Institute for Water Research & Kenya Marine and Fisheries Research Institute*.
616 https://aquadocs.org/bitstream/handle/1834/6965/ktf0339.pdf?sequence=2

Kim, S.-T., & O'Neil, J. R. (1997). Equilibrium and nonequilibrium oxygen isotope effects in synthetic carbonates. *Geochimica et Cosmochimica Acta*, *61*(16), 3461-3475. https://doi.org/10.1016/s0016-7037(97)00169-5

Last, W. M., Teller, J. T., & Forester, R. M. (1994). Paleohydrology and paleochemistry of Lake Manitoba, Canada: the isotope and ostracode records. *Journal of Paleolimnology*, *12*(3), 269-282. https://link.springer.com/article/10.1007/BF00678025

Levin, N. E. (2015). Environment and Climate of Early Human Evolution. *Annual Review of Earth and Planetary Sciences*, *43*(1), 405-429. https://doi.org/10.1146/annurev-earth-060614-105310

Limén, H., & Ólafsson, E. (2002). Ostracod species-specific utilisation of sediment detritus and newly settled cyanobacteria, *Aphanizomenon* sp., in the Baltic Sea: evidence from stable carbon isotopes. *Marine Biology*, *140*(4), 733-738. https://doi.org/10.1007/s00227-001-0739-8

Lupien, R. L., Russell, J. M., Feibel, C., Beck, C., Castañeda, I., Deino, A., & Cohen, A. S. (2018). A leaf wax biomarker record of early Pleistocene hydroclimate from West Turkana, Kenya. *Quaternary Science Reviews*, *186*, 225-235. https://doi.org/10.1016/j.quascirev.2018.03.012

Lupien, R. L., Russell, J. M., Grove, M., Beck, C. C., Feibel, C. S., & Cohen, A. S. (2020). Abrupt climate change and its influences on hominin evolution during the early Pleistocene in the Turkana Basin, Kenya. *Quaternary Science Reviews*, *245*, 106531. https://doi.org/10.1016/j.quascirev.2020.106531

Manobianco, J. A. (2021). Interpretation of Seasonality from Geochemistry and Sclerochronology of Holocene and Pleistocene Freshwater Bivalves from the Omo-Turkana Basin, Ethiopia and Kenya.

Maupin, C. R., Roark, E. B., Thirumalai, K., Shen, C.-C., Schumacher, C., Van Kampen-Lewis, S., Housson, A. L., McChesney, C. L., Baykara, O., Yu, T.-L., White, K., & Partin, J. W. (2021). Abrupt Southern Great Plains thunderstorm shifts linked to glacial climate variability. *Nature Geoscience*. https://doi.org/10.1038/s41561-021-00729-w

Morrissey, A., & Scholz, C. A. (2014). Paleohydrology of Lake Turkana and its influence on the Nile River system. *Palaeogeography, Palaeoclimatology, Palaeoecology*, *403*, 88-100. https://www.sciencedirect.com/science/article/pii/S0031018214001552

Morrissey, A., Scholz, C. A., & Russell, J. M. (2018). Late Quaternary TEX86 paleotemperatures from the world's largest desert lake, Lake Turkana, Kenya. *Journal of Paleolimnology*, *59*(1), 103-117. https://doi.org/10.1007/s10933-016-9939-6

Ng'ang'a, P., Muchane, M. W., Johnson, T. C., & Sturgeon, K. (1998). Comparisrison Of Isotopic Records In Abiogenic And Biogenic Calcite From Lake Turkana, Kenya. In J. T. Lehman (Ed.), *Environmental Change and Response in East African Lakes* (pp. 173-190).

Palacios-Fest, M. R., Cohen, A. S., & Anadón, P. (1994). Use of ostracodes as paleoenvironmental tools in the interpretation of ancient lacustrine records. *Revista Española De Paleontología*, *9*(2), 145-164.

Palacios-Fest, M. R., & Dettman, D. L. (2001). Temperature controls monthly variation in ostracode valve Mg/Ca: Cypridopsis vidua from a small lake in Sonora, Mexico. *Geochimica et Cosmochimica Acta*, *65*(15), 2499-2507. https://www.sciencedirect.com/science/article/pii/S0016703701006020

Pérez, L., Curtis, J., Brenner, M., Hodell, D., Escobar, J., Lozano, S., & Schwalb, A. (2013). Stable isotope values ($\delta^{18}O$ & $\delta^{13}C$) of multiple ostracode species in a large Neotropical

lake as indicators of past changes in hydrology. *Quaternary Science Reviews*, *66*, 96-111. https://doi.org/10.1016/j.quascirev.2012.10.044

Quinn, R. L., & Lepre, C. J. (2020). Revisiting the pedogenic carbonate isotopes and paleoenvironmental interpretation of Kanapoi. *Journal of Human Evolution*, *140*, 102549. https://doi.org/10.1016/j.jhevol.2018.11.005

Ricketts, R. D., & Anderson, R. F. (1998). A direct comparison between the historical record of lake level and the δ¹⁸O signal in carbonate sediments from Lake Turkana, Kenya. *Limnology and Oceanography*. https://aslopubs.onlinelibrary.wiley.com/doi/pdf/10.4319/lo.1998.43.5.0811

Ricketts, R. D., & Johnson, T. C. (1996). Climate change in the Turkana basin as deduced from a 4000 year long δO18 record. *Earth and Planetary Science Letters*, *142*(1-2), 7-17. https://www.sciencedirect.com/science/article/pii/0012821X96000945

Roca, J. R., & Wansard, G. (1997). Temperature influence on development and calcification of Herpetocypris brevicaudata Kaufmann, 1900 (Crustacea: Ostracoda) under experimental conditions. *Hydrobiologia*, *347*(1-3), 91-95. https://link.springer.com/article/10.1023/A:1003067218024

Schwalb, A., Burns, S. J., Cusminsky, G., Kelts, K., & Markgraf, V. (2002). Assemblage diversity and isotopic signals of modern ostracodes and host waters from Patagonia, Argentina. *Palaeogeography, Palaeoclimatology, Palaeoecology*, *187*(3-4), 323-339. https://www.sciencedirect.com/science/article/pii/S0031018202004844

Talbot, M. R. (1990). A review of the palaeohydrological interpretation of carbon and oxygen isotopic ratios in primary lacustrine carbonates. *Chemical Geology: Isotope Geoscience section*, *80*(4), 261-279. https://doi.org/10.1016/0168-9622(90)90009-2

Thirumalai, K., Singh, A., Ramesh, R., & Ramesh, R. (2011). A MATLAB™ code to perform weighted linear regression with (correlated or uncorrelated) errors in bivariate data. *Journal of the Geological Society of India*, *77*(4), 377-380. https://doi.org/10.1007/s12594-011-0044-1

Turpen, J. B., & Angell, R. W. (1971). Aspects of molting and calcification in the ostracod Heterocypris. *The Biological Bulletin*, *140*(2), 331-338. https://www.journals.uchicago.edu/doi/abs/10.2307/1540077

Uno, K. T., Polissar, P. J., Kahle, E., Feibel, C., Harmand, S., Roche, H., & deMenocal, P. B. (2016). A Pleistocene palaeovegetation record from plant wax biomarkers from the Nachukui Formation, West Turkana, Kenya. *Philosophical Transactions of the Royal Society B: Biological Sciences*, *371*(1698), 20150235. https://doi.org/10.1098/rstb.2015.0235

van der Lubbe, H. J. L., Krause-Nehring, J., Junginger, A., Garcin, Y., Joordens, J. C. A., Davies, G. R., Beck, C., Feibel, C. S., Johnson, T. C., & Vonhof, H. B. (2017). Gradual or abrupt? Changes in water source of Lake Turkana (Kenya) during the African Humid Period inferred from Sr isotope ratios. *Quaternary Science Reviews*, *174*, 1-12.

Von Grafenstein, U., Erlernkeuser, H., & Trimborn, P. (1999). Oxygen and carbon isotopes in modern fresh-water ostracod valves: assessing vital offsets and autecological effects of interest for palaeoclimate studies. *Palaeogeography, Palaeoclimatology, Palaeoecology*, *148*(1-3), 133-152. https://www.sciencedirect.com/science/article/pii/S0031018298001801

Vonhof, H. B., Joordens, J. C. A., Noback, M. L., van der Lubbe, J. H. J. L., Feibel, C. S., & Kroon, D. (2013). Environmental and climatic control on seasonal stable isotope variation of freshwater molluscan bivalves in the Turkana Basin (Kenya). *Palaeogeography,*

Palaeoclimatology, Palaeoecology, *383-384*, 16-26. https://doi.org/10.1016/j.palaeo.2013.04.022

Willmott, C. J., & Matsuura, K. (2001). Terrestrial Air Temperature and Precipitation: Monthly and Annual Time Series (1950-1999) (Version 1.02). *Center for Climatic Research, Department of Geography, University of Delaware.*

Wynn, J. G. (2004). Influence of Plio-Pleistocene aridification on human evolution: Evidence from paleosols of the Turkana Basin, Kenya. *American Journal of Physical Anthropology*, *123*(2), 106-118. https://doi.org/10.1002/ajpa.10317

Xia, J., Engstrom, D. R., & Ito, E. (1997). Geochemistry of ostracode calcite: Part 2. The effects of water chemistry and seasonal temperature variation on Candona rawsoni. *Geochimica et Cosmochimica Acta*, *61*(2), 383-391. https://www.sciencedirect.com/science/article/pii/S0016703796003547

York, D., Evensen, N. M., Martínez, M. L., & De Basabe Delgado, J. (2004). Unified equations for the slope, intercept, and standard errors of the best straight line. *American Journal of Physics*, *72*(3), 367-369. https://doi.org/10.1119/1.1632486

Figure Captions

Figure 1. Regional (A) and local (B) setting of Lake Turkana, Kenya. (A) Mean annual precipitation taken from the GPCC dataset (Beck et al. 2005). (B) Satellite imagery of Lake Turkana with labelled sediment samples de- noted in yellow circles. Reference point (red circle) is the marker from which proximity to Omo River inflow is computed.

Figure 2. Temperature (A-B) and rainfall (C-D) climatology and interannual variability over Lake Turkana and adjacent regions. Mean annual values were computed as the average of monthly temperatures over 1900-2017 from the University of Delaware dataset (Willmott & Matsuura, 2001) and rainfall from the GPCC dataset (Beck et al. 2005). Interannual variability was calculated as one standard deviation of annual-mean data from 1900-2017.

Figure 3. Stable carbon and oxygen isotope analyses of ostracodes at Lake Turkana from this study (blue) and previous studies (colors). (A) $\delta^{18}O$ vs $\delta^{13}C$ (‰, VPDB) of various species of ostracodes (differ- ent species indicated by shape) in Lake Turkana reported in previous work and this study (blue circles). Note that measurements presented in this study are on individual valves whereas the previous studies represent multi-specimen analyses. (B) $\delta^{18}O$ vs $\delta^{13}C$ of specimens pooled by location in our study. Regression statistics reported in each subplot were conducted using Maximum Likelihood Estimation using bivariate uncertainty (see Methods for details).

Figure 4. Average IOVA-$\delta^{13}C$ (A) and -$\delta^{18}O$ (B) in surface sediments from Lake Turkana as a function of proximity to Omo River inflow. Each data point represents the average of all measurements on *S. clavularis* at each site and values are reported with respect to the VPDB scale (‰). Distance from Omo River inflow was assigned based on a fixed reference point (see Methods and Fig. 1 for details), and regression statistics were performed using Maximum Likelihood Estimation. Errorbars represent combined root mean square errors of analytical precision and intra-site isotopic variance.

Figure 5. (A) Comparison of $\delta^{18}Ow$ in Lake Turkana measured in 1994 versus those reconstructed using individual ostracode valve analyses (IOVA) from samples collected in 1979 along with (B) annual rainfall anomaly between 1994 and 1979. (A) $\delta^{18}Ow$ measurements (green circles) were taken from Ricketts and Johnson (1998) whereas IOVA-based $\delta^{18}Ow$ was reconstructed using IOVA-$\delta^{18}O$ and *in situ* bottom-water temperature measurements (Cohen, 1986) based on equilibrium isotope fractionation (see Methods for details). Dashed lines depict linear regression lines of best fit (York et al. 2004) and errors represent root mean square values of analytical precision and intra-site IOVA-$\delta^{18}O$ variance. (B) Rainfall anomaly of mean annual precipitation between 1993 and 1979 from the GPCC dataset (Beck et al. 2005).

766 **Table 1.** Inter-site mean individual ostracode valve analyses (IOVA) of stable isotopes and valve characteristics (mass, length – L1,
767 width – L2) and *in situ* environmental parameters including pH, surface water and bottom water temperatures at site locations as well
768 as distance of site from a fixed marker in the Omo River inflow region (see Fig. 2). NA indicates not available.

Site #	Site ID	Lat (°N)	Lon (°E)	Depth (m)	Dist. (km)	pH	Sur. T (°C)	Bot. T (°C)	# IOVA	Avg. Mass (µg)	1σ Mass (µg)	Avg. L1 (µm)	1σ L1 (µm)	Avg. L2 (µm)	1σ L2 (µm)	Avg. $\delta^{13}C$ (‰)	1σ $\delta^{13}C$ (‰)	Avg. $\delta^{18}O$ (‰)	1σ $\delta^{18}O$ (‰)
1	BS125	4.3613	36.1988	1	50.0	9.1	NA	NA	13	166	39	2078	115	1074	219	-2.88	1.09	2.49	0.45
2	79-170F	4.2061	35.9535	14.5	65.0	9.1	27	26	22	249	36	2135	50	1124	33	-1.82	0.84	2.85	0.38
3	BS91	4.1369	36.2127	0.5	74.4	7.6	NA	NA	19	228	24	2085	71	1065	49	-2.21	1.23	3.15	0.43
4	BS90	4.1215	36.2179	0.2	76.4	10.3	NA	NA	15	218	48	2078	121	1030	143	-2.25	1.12	3.06	0.53
5	79-168F	4.0717	35.9230	15	80.6	9.1	27.5	23.5	21	230	42	2107	86	1105	53	-1.53	0.77	3.30	0.44
6	79-166F	3.9491	35.8664	10	94.8	9.1	29	27	15	194	37	2073	103	1087	31	-2.44	0.68	3.00	0.28
7	79-147F	3.7723	36.2214	9.5	114.3	9	25	24.7	21	156	57	1966	196	990	56	-1.22	1.10	3.40	0.53
8	79-164F	3.7386	35.8532	15.5	118.3	9.1	30	26.9	19	194	29	2055	79	1078	32	-1.49	1.19	3.25	0.31
9	79-130F	3.5659	35.9087	22	136.2	NA	27	26	21	228	33	2092	84	1106	51	-2.00	1.15	3.19	0.53
10	79-77F	3.5417	35.9589	29	138.4	8.7	NA	NA	20	237	26	2021	226	1150	214	-1.75	0.87	3.41	0.31
11	79-158F	3.4792	36.0490	27	145.0	9.1	NA	NA	21	277	35	2131	77	1117	47	-2.35	0.88	3.01	0.31
12	79-160F	3.4407	36.1774	37	150.0	NA	NA	NA	22	273	28	2137	66	1094	40	-0.95	0.83	3.62	0.38
13	79-183F	3.3115	36.0044	21	163.6	NA	NA	NA	20	238	45	2096	95	1095	49	-1.16	1.32	3.48	0.55
14	79-189F	3.0290	36.2264	31	195.7	NA	NA	NA	20	213	27	2036	76	1077	34	-1.80	1.12	3.55	0.32
15	79-204F	2.8216	36.6274	59	227.0	NA	NA	NA	23	220	49	2137	91	1127	63	-1.75	1.24	4.20	0.38
16	79-193F	2.7819	36.4219	59	226.0	NA	NA	NA	17	250	41	2107	127	1105	94	-1.51	0.79	3.96	0.57
17	79-194F	2.7380	36.5046	62	240.0	NA	NA	NA	18	222	43	2080	117	1108	80	-0.61	0.71	4.51	0.49
					Average	9.0	27.6	25.7	19.2	223	38	2083	105	1090	76	-1.75	1.00	3.38	0.42
					1 σ	0.6	1.7	1.4	2.8	32	9	45	45	38	60	0.58	0.21	0.50	0.10

769

Table 2. Coefficient of determination (r^2) matrix between measured IOVA parameters pooled across sites including valve characteristics (see Table 1 for abbreviations), $\delta^{18}O$, $\delta^{13}C$, and their $1\sigma_{intra}$ variability with each other and with latitude, longitude, depth, and distance from Omo River inflow. Note that correlations with pH and temperature measurements were not performed due to incomplete datasets (Table 1). Asterisks (*) delineate r^2 values significant at the $p<0.001$ level.

	Avg. Mass	Avg. L1	Avg. L2	$\delta^{13}C$	$\delta^{13}C$ 1σ	$\delta^{18}O$	$\delta^{18}O$ 1σ
Distance	0.08	0.01	0.11	0.33*	0.00	0.81*	0.01
Latitude	0.09	0.01	0.12	0.32*	0.00	0.78*	0.01
Longitude	0.00	0.01	0.01	0.06	0.01	0.46*	0.11
Depth	0.16*	0.09	0.27*	0.32*	0.08	0.78*	0.00
Avg. Mass	x	x	x	x	x	x	x
Avg. L1	0.49*	x	x	x	x	x	x
Avg. L2	0.40*	0.32*	x	x	x	x	x
$\delta^{13}C$	0.04	0.00	0.00	x	x	x	x
$\delta^{13}C$ 1σ	0.08	0.03	0.12	0.02	x	x	x
$\delta^{18}O$	0.04	0.00	0.05	0.56*	0.01	x	x
$\delta^{18}O$ 1σ	0.01	0.00	0.13	0.07	0.05	0.04	x

Table 3. Investigation of oxygen isotope equilibrium of IOVA-$\delta^{18}O$ calcification. Comparisons of measured versus calculated limnological parameters where $\delta^{18}O_w$ was computed using IOVA-$\delta^{18}O$ averages and measured bottom water temperature in Eqn. (1), whereas bottom water temperature was calculated using average IOVA-$\delta^{18}O$ and measured $\delta^{18}O_w$. Errors (reported as ± 1σ) were propagated in the calculated values using a Monte Carlo procedure based on a root mean square combination of sampling (*i.e.,* intra-site 1σ) and analytical uncertainty.

Domain	Avg. IOVA-$\delta^{18}O$ (‰, VPDB)	*n*	Measured $\delta^{18}O_w$ (‰, VSMOW)	*n*	Measured Bot. T (°C)	*n*	Calculated $\delta^{18}O_w$ (‰, VSMOW)	Calculated Bot. T (°C)
North of 3.9°N	2.98 ± 0.28	105	5.86 ± 0.56	19	25.3 ± 1.5	4	5.96 ± 0.3	25.3 ± 2.8
Koobi Fura Spit	3.11 ± 0.5	34	5.74 ± 0.57	17	23.5	1	5.73 ± 0.51	23.6 ± 3.2
All Samples	3.40 ± 0.62	329	5.72 ± 0.71	37	25.7 ± 1.4	6	6.4 ± 0.5	22.5 ± 3.8